Journal of Solid State Chemistry **163,** 194–201 (2002)
doi:10.1006/jssc.2001.9392, available online at http://www.idealibrary.com on IDEAL®

The Crystal Chemistry of Lithium in the Alluaudite Structure: A Study of the $(Na_{1-x}Li_x)CdIn_2(PO_4)_3$ Solid Solution ($x = 0$ to 1)

Frédéric Hatert,*,[1] Diano Antenucci,† André-Mathieu Fransolet,* and Monique Liégeois-Duyckaerts‡

*Laboratoire de Minéralogie, Université de Liège, B-4000 Liège, Belgium; †Institut Scientifique de Service Public, B-4000 Liège, Belgium; and ‡Institut de Chimie, Université de Liège, B-4000 Liège, Belgium

Received April 30, 2001; in revised form August 28, 2001; accepted September 7, 2001

Several compounds of the $(Na_{1-x}Li_x)CdIn_2(PO_4)_3$ solid solution were synthesized by a solid-state reaction in air, and pure alluaudite-like compounds were obtained for $x = 0.00$, 0.25, and 0.50. X-ray Rietveld refinements indicate the occurrence of Cd^{2+} in the $M(1)$ site, and of In^{3+} in the $M(2)$ site of the alluaudite structure. This non-disordered cationic distribution is confirmed by the sharpness of the infrared absorption bands. The distribution of Na^+ and Li^+ on the $A(1)$ and $A(2)'$ crystallographic sites cannot be accurately assessed by the Rietvled method, probably because the electronic densities involved in the $Na^+ \rightarrow Li^+$ substitution are very small. A comparison with the synthetic alluaudite-like compounds, $(Na_{1-x}Li_x)MnFe_2(PO_4)_3$, indicates the influence of the cations occupying the $M(1)$ and $M(2)$ sites on the coordination polyhedra morphologies of the $A(1)$ and $A(2)'$ crystallographic sites. © 2002 Elsevier Science

Key Words: **$(Na_{1-x}Li_x)CdIn_2(PO_4)_3$; alluaudite structure type; solid-state reaction synthesis; X-ray Rietveld refinement; infrared spectroscopy.**

INTRODUCTION

The alluaudite structure (monoclinic $C2/c$, $Z = 4$) was first determined by Moore (1) on a natural specimen from the Buranga pegmatite, Rwanda. Its general structural formula was recently reformulated as $[A(2)A(2)'][A(1)A(1)'A(1)''_2]M(1)M(2)_2(PO_4)_3$ (2). In natural alluaudites, the large crystallographic A sites are occupied by Na^+, Ca^{2+}, or Mn^{2+}, and the distorted octahedral M sites are occupied by Mn^{2+}, Fe^{2+}, Fe^{3+}, Al^{3+}, or Mg^{2+} (3).

Over the past decade, the family of phosphate and arsenate compounds exhibiting an alluaudite-like structure has been considerably extended. By solid-state reactions, exotic cations have been inserted into the alluaudite framework. Antenucci *et al.* (4, 5) have shown that the $M(2)$ sites can accept In^{3+}, Ga^{3+}, and Cr^{3+} and that the $M(1)$ site can accept Cd^{2+}. Some analogous synthetic arsenates have been reported with the $M(2)$ site occupied by Ni^{2+} and Co^{2+} (6, 7) or, in some cases, by In^{3+} (8, 9). New mixed-valence compounds have also been prepared, such as Cu^+ and Cu^{2+} in $Cu_{1.35}Fe_3(PO_4)_3$ or $Cu_2Mg_3(PO_4)_3$ (10), Fe^{2+} and Fe^{3+} in $Na_2Fe_3(PO_4)_3$ (11), and more recently in $NaFe_{3.67}(PO_4)_3$ (12). In contrast with these hydrogen-free compounds, new protonated groups of alluaudite-like phosphate (13–16) and arsenate compounds (14, 17) have also been reported.

Although these experimental studies led to a better understanding of the crystallochemical role of a large number of cations in the alluaudite structure, the behavior of lithium is scarcely envisaged. Recently, lithium was inserted in the arsenate solid solution, $(Na_{1-x}Li_x)_3Fe_2^{3+}(AsO_4)_3$ (18). Pure alluaudite-like compounds were obtained in the $0.333 \leq x \leq 0.666$ compositional range, but the distribution model of lithium on the different crystallographic sites of the alluaudite structure was not supported by any structural refinement.

Because alluaudite occurs in late magmatic geochemically lithium-rich environments, and because this mineral usually contains small amounts of Li^+, up to 0.30 atoms per formula unit (3), the crystallochemical role of lithium in the alluaudite structure looks like an enigmatic question. This is why Hatert *et al.* (2) examined the role of lithium in the synthetic $(Na_{1-x}Li_x)MnFe_2(PO_4)_3$ series. The aim of this paper is to extend the earlier experimental study (2) to the $(Na_{1-x}Li_x)CdIn_2(PO_4)_3$ solid solution, in order to elucidate the crystal chemistry of lithium when Mn^{2+} and Fe^{3+} are replaced by different cations.

EXPERIMENTAL

Compounds of the $(Na_{1-x}Li_x)CdIn_2(PO_4)_3$ solid solution were synthesized by solid-state reactions in air.

[1]To whom correspondence should be addressed. E-mail: fhatert@ulg.ac.be. Fax: 0032-4-366.22.02.

0022-4596/02 $35.00

Stoichiometric quantities of $NaHCO_3$, Li_2CO_3, $CdCO_3$, In_2O_3, and $NH_4H_2PO_4$ were dissolved in concentrated nitric acid, and the resulting solution was evaporated to dryness. The dry residue was progressively heated for 15 to 20 hours in a platinum crucible, to the temperature of 950°C. Alluaudite-like compounds were obtained by quenching the product in air.

X-ray powder diffraction patterns were recorded on a PHILIPS PW-3710 diffractometer using Fe$K\alpha$ radiation, with $\lambda = 1.9373$ Å. The unit cell parameters were calculated with the least-squares refinement program LCLSQ 8.4 (19), from the *d*-spacings calibrated with an internal standard of $Pb(NO_3)_2$. The starting parameters used for the Rietveld refinements of the alluaudite-like compounds, $(Na_{1-x}Li_x)CdIn_2(PO_4)_3$, with $x = 0.00$, 0.25, and 0.50, were the unit cell parameters calculated from the $Pb(NO_3)_2$-calibrated powder patterns, and the atomic positions given for $NaCdIn_2(PO_4)_3$ (5). Experimental details for the Rietveld refinements are presented in Table 1, and the final Rietveld plot for $Na_{0.50}Li_{0.50}CdIn_2(PO_4)_3$ is shown in Fig. 1. Fits of equivalent quality were obtained for the other compounds.

Infrared spectra were recorded with a Nicolet MAGNA-IR 760 spectrometer over the 400–4000 cm^{-1} region, in KBr discs, or with a Bruker IFS 66 spectrometer over the 100–550 cm^{-1} region, in polyethylene discs. In order to observe isotopic frequency shifts, alluaudite-like compounds were synthesized from 96% isotopically pure $^6Li_2CO_3$.

TABLE 1
Experimental Details for the Rietveld Refinements of $(Na_{1-x}Li_x)CdIn_2(PO_4)_3$

	x		
	0.00	0.25	0.50
Rietveld program		DBWS-9807 (29)	
2θ range (Fe$K\alpha$)		10–100	
Step width (°2θ Fe$K\alpha$)		0.02	
Step time (s)		15	
Number of reflexions	539	539	532
Refined Parameters			
Structural parameters			
Positional	27	27	27
Population	4	4	4
Thermal	4	4	5
Cell parameters	4	4	4
Background	5	5	5
Profile	6	6	6
Zero point (°2θ)	1	1	1
Scale factor	1	1	1
Preferred orientation (011)	1	1	1
Sample parameters	2	2	2
Total	55	55	56
R_p (%)	5.96	5.80	5.92
R_{wp} (%)	8.13	7.77	7.83
$R_{exp.}$ (%)	3.31	3.27	3.26
$R_{(Bragg)}$ (%)	3.20	3.24	3.59
S	2.44	2.36	2.39

RESULTS AND DISCUSSION

Characterization of the Compounds

The $(Na_{1-x}Li_x)CdIn_2(PO_4)_3$ alluaudite-like compounds crystallize in a fine-grained white powder. X-ray powder diffraction patterns show that pure alluaudite-like phases are obtained for *x* extending from 0.00 to 0.50. In the range $0.60 \leq x \leq 1.00$, the alluaudite-like phase is intimately mixed with $Li_3In_2(PO_4)_3$ (20). Thus, the maximum amount of lithium which may be inserted in the $(Na_{1-x}Li_x)CdIn_2(PO_4)_3$ solid solution must be between $x = 0.50$ and $x = 0.60$; herein we arbitrarily choose $x = 0.55$.

X-Ray Rietveld Refinements of $(Na_{1-x}Li_x)CdIn_2(PO_4)_3$

The atomic parameters and the interatomic distances and angles, deduced from the Rietveld refinements of the $(Na_{1-x}Li_x)CdIn_2(PO_4)_3$ compounds, with $x = 0.00$, 0.25, and 0.50, are presented in Tables 2 and 3, respectively. The satisfactory values of R_p, R_{wp}, R_{Bragg}, and *S* (Table 1) confirm the reliability of the refinements, as well as the mean O–P(1)–O and O–P(2)–O angles that are very close to those of an ideal tetrahedron (Table 3). A polyhedral representation of the crystal structure of $Na_{0.50}Li_{0.50}CdIn_2(PO_4)_3$, approximately projected along [001], is shown in Fig. 2.

The positional parameters of the alluaudite-like compounds (Table 2) correspond to the $A(2)'$, $A(1)$, $M(1)$, and $M(2)$ crystallographic sites, labeled according to the nomenclature recently proposed by Hatert *et al.* (2). The coordination polyhedra morphologies of $M(1)$, which is a very distorted octahedron, and of $M(2)$, which is a distorted octahedron, are similar to the morphologies previously described for the $(Na_{1-x}Li_x)MnFe_2(PO_4)_3$ compounds (2), whereas the $A(1)$ and $A(2)'$ sites do not resemble the distorted cube and the gable disphenoid, respectively. Excluding the $A(1)$–O(2) and $A(2)'$–O(1) bonds longer than 3.0 Å, a morphology corresponding to a distorted octahedron is observed for the $A(1)$ site (Fig. 3a), whereas the $A(2)'$ site exhibits a 4 + 2 coordination, with four short bonds and two long bonds (Table 3). This coordination polyhedron corresponds to a distorted trigonal prism (Fig. 3b), very similar to that described in the synthetic alluaudite-like compound, $NaCaCdMg_2(PO_4)_3$ (21).

The mechanisms involved in the insertion of lithium into the $(Na_{1-x}Li_x)CdIn_2(PO_4)_3$ alluaudite-like compounds are difficult to establish, because the electronic densities occurring on the $A(1)$ and $A(2)'$ crystallographic sites are very small. For $NaCdIn_2(PO_4)_3$, the occupancy factors (Table 2)

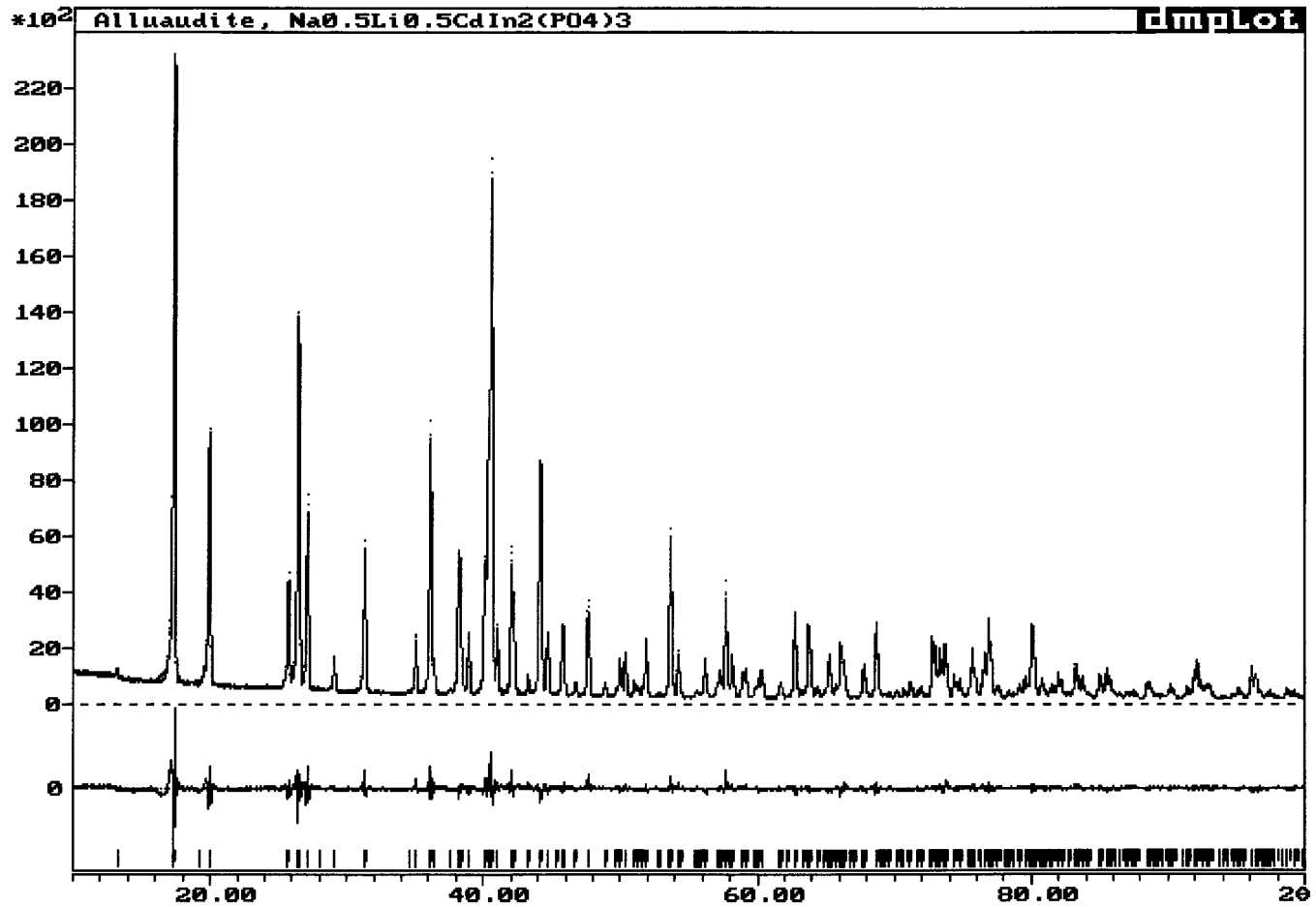

FIG. 1. Final Rietveld plot showing the observed (dots), calculated (solid line), and difference patterns for $Na_{0.50}Li_{0.50}CdIn_2(PO_4)_3$. The vertical markers indicate the positions calculated for $K\alpha_1$ and $K\alpha_2$ Bragg reflexions.

indicate that Na^+ occupies the $A(1)$ crystallographic site, as already demonstrated by Antenucci *et al.* (5). An electronic density, attributed to Na^+, has also been detected on a position which corresponds to the $A(2)'$ crystallographic site. The X-ray powder diffraction patterns of $Na_{0.75}Li_{0.25}CdIn_2(PO_4)_3$ and $Na_{0.50}Li_{0.50}CdIn_2(PO_4)_3$ were refined using a model with Li^+ localized on the $A(1)$ site. When the lithium content of the $A(1)$ site is fixed to its theoretical value, the occupancy factors of Na^+ are very close to the ideal composition (Table 2). Nevertheless, two other models can also be considered with lithium occurring on the $A(2)'$ site, or with this cation distributed between the $A(1)$ and $A(2)'$ crystallographic sites. The similar values of R_p, R_{wp}, R_{Bragg}, and S for these alternative models indicate that the distribution of Na^+ and Li^+ on the $A(1)$ and $A(2)'$ crystallographic sites cannot be accurately assessed with the Rietveld method.

For the cationic distribution on the M sites, the occupancy factors (Table 2) indicate the occurrence of Cd^{2+} on $M(1)$ and of In^{3+} on $M(2)$. This non-disordered distribution is in good agreement with the $M(1)$–O and $M(2)$–O average distances (Table 3), which are very close to the interatomic Cd^{2+}–O and In^{3+}–O distances of 2.35 and 2.20 Å, respectively (22). The bond valence sums for these sites have also been calculated using the empirical parameters of Brown and Altermatt (23). According to these authors, the bond valence, s, associated with the bond length, R, is given by the equation $s = \exp[(R_0 - R)/0.37]$, where R_0 is 1.904 for Cd^{2+} and 1.902 for In^{3+}. Ideally, the bond valence sum should equal the mean valence of the cation in a crystallographic site. For full Cd^{2+} occupation on $M(1)$ ($\sum_s = 1.87$–1.89), and for full In^{3+} occupation on $M(2)$ ($\sum_s = 3.09$–3.20), the bond valence sums are very close to the ideal value, thus confirming the non-disordered distribution of Cd^{2+} and In^{3+} on the $M(1)$ and $M(2)$ sites.

Variation of the Unit Cell Parameters

The unit cell parameters of the different members of the $(Na_{1-x}Li_x)CdIn_2(PO_4)_3$ series (Table 4) show a regular

TABLE 2
Positional (x, y, z), Isotropic Thermal (B), and Site Occupancy (N) Parameters for $(Na_{1-x}Li_x)CdIn_2(PO_4)_3$

Site	Atom	Wyckoff	x	y	z	B(Å^2)	N
				$NaCdIn_2(PO_4)_3$			
$A(2)'$	Na	4*e*	0	0.019(7)	0.25	1.00	0.053(6)
$A(1)$	Na	4*b*	0.50	0	0	3.9(5)	0.55(1)
$M(1)$	Cd	4*e*	0	0.2624(2)	0.25	0.4(1)	0.474(3)
$M(2)$	In	8*f*	0.2803(1)	0.6504(1)	0.3687(3)	0.45(6)	0.974(7)
P(1)	P	4*e*	0	− 0.2858(7)	0.25	1.00	0.50
P(2)	P	8*f*	0.2428(5)	− 0.1094(4)	0.141(1)	1.00	1.00
O(1)	O	8*f*	0.453(1)	0.7161(8)	0.543(2)	0.8(1)	1.00
O(2)	O	8*f*	0.094(1)	0.640(1)	0.238(2)	0.8(1)	1.00
O(3)	O	8*f*	0.3286(9)	0.6583(9)	0.101(2)	0.8(1)	1.00
O(4)	O	8*f*	0.128(1)	0.4008(8)	0.324(2)	0.8(1)	1.00
O(5)	O	8*f*	0.2287(9)	0.8214(8)	0.318(2)	0.8(1)	1.00
O(6)	O	8*f*	0.3113(9)	0.4947(9)	0.359(2)	0.8(1)	1.00
				$Na_{0.75}Li_{0.25}CdIn_2(PO_4)_3$			
$A(2)'$	Na	4*e*	0	0.029(5)	0.25	1.00	0.073(6)
$A(1)$	Na	4*b*	0.50	0	0	4.7(7)	0.36(1)
	Li	4*b*	0.50	0	0	4.7(7)	0.125
$M(1)$	Cd	4*e*	0	0.2650(2)	0.25	1.0(1)	0.484(3)
$M(2)$	In	8*f*	0.2793(1)	0.6505(1)	0.3662(3)	0.11(5)	0.956(6)
P(1)	P	4*e*	0	− 0.2881(6)	0.25	1.00	0.50
P(2)	P	8*f*	0.2425(5)	− 0.1097(4)	0.138(1)	1.00	1.00
O(1)	O	8*f*	0.4525(9)	0.7186(8)	0.546(2)	0.7(1)	1.00
O(2)	O	8*f*	0.0922(9)	0.6413(9)	0.231(2)	0.7(1)	1.00
O(3)	O	8*f*	0.3266(9)	0.6599(9)	0.106(2)	0.7(1)	1.00
O(4)	O	8*f*	0.1274(9)	0.4013(7)	0.322(1)	0.7(1)	1.00
O(5)	O	8*f*	0.2271(8)	0.8222(8)	0.317(2)	0.7(1)	1.00
O(6)	O	8*f*	0.3189(8)	0.4927(8)	0.367(2)	0.7(1)	1.00
				$Na_{0.50}Li_{0.50}CdIn_2(PO_4)_3$			
$A(2)'$	Na	4*e*	0	− 0.001(6)	0.25	1.00	0.060(6)
$A(1)$	Na	4*b*	0.50	0	0	7(1)	0.26(1)
	Li	4*b*	0.50	0	0	7(1)	0.25
$M(1)$	Cd	4*e*	0	0.2647(2)	0.25	0.62(9)	0.492(4)
$M(2)$	In	8*f*	0.2796(1)	0.6501(1)	0.3664(3)	0.32(5)	0.993(8)
P(1)	P	4*e*	0	− 0.2878(6)	0.25	0.1(1)	0.50
P(2)	P	8*f*	0.2422(4)	− 0.1096(4)	0.1370(9)	0.1(1)	1.00
O(1)	O	8*f*	0.4527(9)	0.7174(8)	0.542(2)	0.2(2)	1.00
O(2)	O	8*f*	0.0915(8)	0.6371(9)	0.230(2)	0.2(2)	1.00
O(3)	O	8*f*	0.3242(8)	0.6628(8)	0.097(2)	0.2(2)	1.00
O(4)	O	8*f*	0.1267(9)	0.4042(7)	0.319(1)	0.2(2)	1.00
O(5)	O	8*f*	0.2261(8)	0.8237(7)	0.315(2)	0.2(2)	1.00
O(6)	O	8*f*	0.3159(8)	0.4909(8)	0.369(2)	0.2(2)	1.00

decrease with increasing x, resulting from the replacement of Na^+ by Li^+ on the crystallographic A sites (Fig. 4). For $x \geq 0.55$, the constant values of the parameters indicate that additional Li^+ could not be incorporated into the structure, which implies the formation of $Li_3In_2(PO_4)_3$ as an additional phase.

The decrease of the unit cell parameters can also be correlated with the variation of bond distances induced by the incorporation of lithium into the alluaudite structure. The differences between the bond lengths of $NaCdIn_2(PO_4)_3$ and $Na_{0.50}Li_{0.50}CdIn_2(PO_4)_3$, presented in Table 3, clearly indicate that significant variations in the bond distances occur for the $A(1)$ and $A(2)'$ crystallographic sites. Important variations are observed for the $A(1)$–O(2) and $A(1)$-O(4) bonds, forming a square parallel to the b axis (Fig. 3a). This feature explains the significant decrease in the b parameter (Fig. 4). In the same way, the smaller variation of the a unit cell parameter is probably related to the shortening of the $A(2)'$–O(6) bonds, forming a square parallel to (010) (Fig. 3b). It is very important to note that the increase of the $A(2)'$–O(3) bond distances is compensated by the decrease of the $A(2)'$–O(1) bond distances (Table 3).

TABLE 3
Interatomic Distances (Å) and Angles (°) for $(Na_{1-x}Li_x)CdIn_2(PO_4)_3$

	x			
	0.00	0.25	0.50	Difference
$A(2)'$–O(6) 2×	2.65(1)	2.58(1)	2.569(9)	− 0.08
$A(2)'$–O(3) 2×	2.65(6)	2.59(4)	2.90(5)	+ 0.25
$A(2)'$–O(6) 2×	2.77(1)	2.73(1)	2.729(7)	− 0.04
$A(2)'$–O(1) 2×	3.28(9)	3.34(5)	3.06(7)	− 0.22
Mean	2.84	2.81	2.81	− 0.03
$A(1)$–O(2) 2×	2.36(1)	2.34(1)	2.29(1)	− 0.07
$A(1)$–O(4) 2×	2.42(1)	2.399(9)	2.360(8)	− 0.06
$A(1)$–O(4) 2×	2.672(9)	2.671(8)	2.658(8)	− 0.01
$A(1)$–O(2) 2×	3.07(1)	3.091(9)	3.054(9)	− 0.02
Mean	2.63	2.63	2.59	− 0.04
$M(1)$–O(4) 2×	2.31(1)	2.286(9)	2.309(9)	− 0.00
$M(1)$–O(1) 2×	2.32(1)	2.341(9)	2.317(9)	− 0.00
$M(1)$–O(3) 2×	2.363(9)	2.384(9)	2.378(8)	+ 0.02
Mean	2.33	2.34	2.33	0.00
$M(2)$–O(6)	2.06(1)	2.10(1)	2.10(1)	+ 0.04
$M(2)$–O(3)	2.09(1)	2.038(9)	2.081(9)	− 0.01
$M(2)$–O(2)	2.112(8)	2.119(7)	2.128(6)	+ 0.02
$M(2)$–O(5)	2.14(1)	2.148(9)	2.151(9)	+ 0.01
$M(2)$–O(1)	2.146(9)	2.159(8)	2.145(8)	− 0.00
$M(2)$–O(5)	2.29(1)	2.30(1)	2.322(9)	+ 0.03
Mean	2.14	2.14	2.15	+ 0.01
P(1)–O(1) 2×	1.53(1)	1.51(1)	1.53(1)	0.00
P(1)–O(2) 2×	1.55(1)	1.52(1)	1.55(1)	0.00
Mean	1.54	1.52	1.54	0.00
O(2)–P(1)–O(2)	103.7(8)	106.0(7)	102.3(7)	
O(1)–P(1)–O(1)	107.4(8)	106.9(7)	107.3(7)	
O(2)–P(1)–O(1) 2×	109.1(5)	107.9(5)	108.1(5)	
O(2)–P(1)–O(1) 2×	113.8(5)	114.2(5)	115.7(5)	
Mean	109.5	109.5	109.5	
P(2)–O(6)	1.51(1)	1.53(1)	1.48(1)	− 0.03
P(2)–O(4)	1.539(9)	1.538(8)	1.544(8)	+ 0.01
P(2)–O(5)	1.54(1)	1.55(1)	1.54(1)	0.00
P(2)–O(3)	1.58(1)	1.60(1)	1.56(1)	− 0.02
Mean	1.54	1.55	1.53	− 0.01
O(4)–P(2)–O(3)	107.0(5)	106.7(5)	107.8(4)	
O(6)–P(2)–O(3)	107.3(7)	106.4(6)	108.4(6)	
O(6)–P(2)–O(5)	108.9(6)	106.6(5)	106.8(5)	
O(5)–P(2)–O(3)	109.1(6)	110.0(6)	108.4(6)	
O(6)–P(2)–O(4)	111.5(6)	114.1(5)	111.8(5)	
O(4)–P(2)–O(5)	112.9(6)	112.9(5)	113.5(5)	
Mean	109.5	109.5	109.5	

Consequently, these variations of bond distances do not affect significantly the unit cell parameters.

Infrared Spectroscopy

The infrared spectrum of $Na_{0.50}Li_{0.50}CdIn_2(PO_4)_3$ (Fig. 5) is very similar to that of $NaCdIn_2(PO_4)_3$ and exhibits the same complexity, which is related to the low symmetry and to the large unit cell of the alluaudite structure (5). A comparison with the infrared spectra of the alluaudite-like $(Na_{1-x}Li_x)MnFe_2(PO_4)_3$ compounds shows the sharpness of the bands for the indium-bearing compounds, particularly obvious in the low-frequency region of the spectrum. This feature was already noted by Antenucci *et al.* (5), who compared the spectra of $NaCdIn_2(PO_4)_3$ with that of the natural alluaudite from the Buranga pegmatite, Rwanda. The sharpness of the bands likely results from the non-disordered distribution of cations on the $M(1)$ and $M(2)$ crystallographic sites of the indium-bearing alluaudites, whereas the iron-bearing alluaudites accommodate Fe^{2+} and Fe^{3+} on their $M(2)$ crystallographic site (2, 24).

Most of the band assignments previously proposed for $NaCdIn_2(PO_4)_3$ (5) can be extended to the Li-bearing

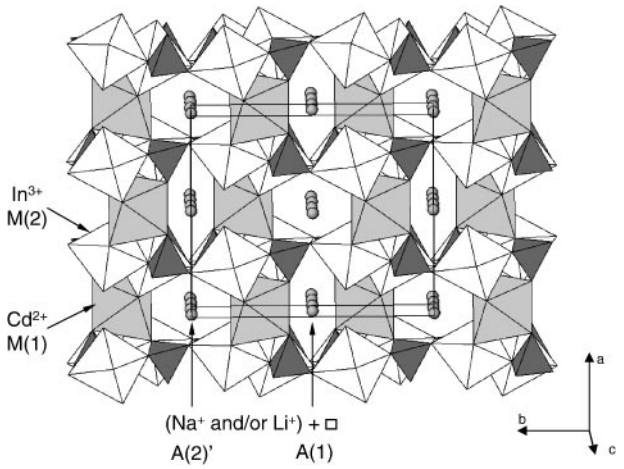

FIG. 2. Projection of the crystal structure of $Na_{0.50}Li_{0.50}CdIn_2(PO_4)_3$. The PO_4 tetrahedra are densely shaded. The shaded $M(1)$ octahedra are occupied by Cd^{2+}, the unshaded $M(2)$ octahedra by In^{3+}. The circles indicate Na^+ and/or Li^+ on the $A(2)'$ and $A(1)$ crystallographic sites.

TABLE 4
Unit Cell Parameters for the Synthetic Alluaudite-like Compounds, $(Na_{1-x}Li_x)CdIn_2(PO_4)_3$

x	a (Å)	b (Å)	c (Å)	β (°)	Vol. (Å^3)
0.00	12.517(3)	12.966(3)	6.571(2)	115.36(2)	963.7(3)
0.25	12.502(2)	12.944(2)	6.572(1)	115.44(2)	960.4(2)
0.50	12.479(2)	12.917(2)	6.571(1)	115.55(1)	955.6(2)
0.60[a]	12.474(3)	12.909(2)	6.573(1)	115.61(1)	954.5(2)
0.70[a]	12.470(2)	12.907(2)	6.575(1)	115.64(1)	954.1(2)
0.75[a]	12.472(2)	12.905(2)	6.574(1)	115.67(1)	953.8(2)
1.00[a]	12.476(3)	12.906(3)	6.571(2)	115.74(2)	953.0(3)

[a]Alluaudite + $Li_3In_2(PO_4)_3$.

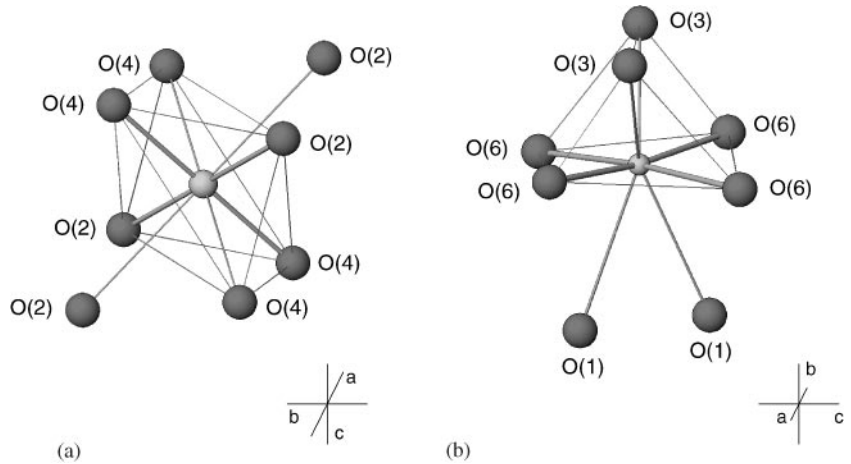

FIG. 3. Morphology of the $A(1)$ (a) and $A(2)'$ (b) crystallographic sites in the alluaudite-like compound, $Na_{0.50}Li_{0.50}CdIn_2(PO_4)_3$.

compound. Nevertheless, in view of the peculiar coordination of lithium in $Na_{0.50}Li_{0.50}CdIn_2(PO_4)_3$, it is of interest to attempt an identification of the Li–O absorption bands by mean of the ^6Li–^7Li isotopic frequency shifts (25, 26). The spectra show one weak band shifting from 432 to 445 cm^{-1} (Fig. 5), when natural lithium (essentially ^7Li) is replaced by ^6Li. The moderate frequency shift of 13 cm^{-1} is lower than that theoretically predicted (27), thus indicating the probable occurrence of interactions between the Li-O vibrations and other internal PO_4 bending vibrations or external modes.

By using the data collected from the literature, we attempted to correlate the Li–O bond length with the corresponding vibrational frequency (Table 5). However, there is no obvious correlation, and the frequency range observed for $Na_{0.50}Li_{0.50}CdIn_2(PO_4)_3$ cannot be considered as characteristic for a given Li–O bond length.

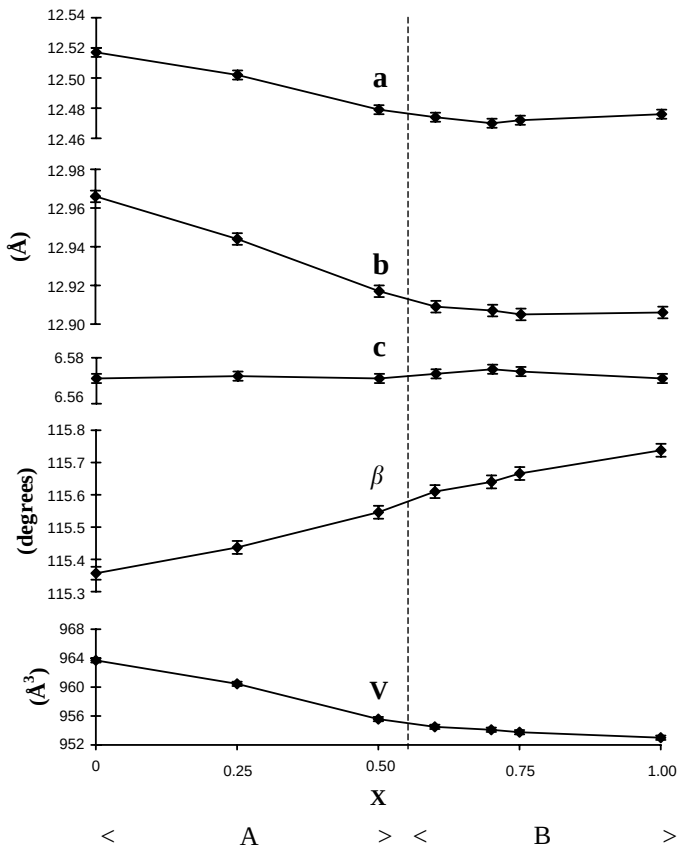

FIG. 4. Variation of the unit cell parameters for the synthetic alluaudite-like compounds, $(Na_{1-x}Li_x)CdIn_2(PO_4)_3$. (A) pure alluaudite; (B) alluaudite + $Li_3In_2(PO_4)_3$.

CONCLUSIONS

The crystallochemical study of the $(Na_{1-x}Li_x)CdIn_2(PO_4)_3$ solid solution, compared with that of $(Na_{1-x}Li_x)MnFe_2(PO_4)_3$ (2), confirms that lithium is not localized on the small $M(2)$ site of the alluaudite structure, as suggested by Moore (1). Due to the very small electronic

TABLE 5
Literature Values of the Li–O Bond Distances and Corresponding Infrared Absorption Bands

Compound	Coordination	Li–O distance (Å)	Wavenumber (cm^{-1})	Refs.
Li_2CO_3	[4]	1.96–2.00	397–497	25, 30
Li_2WO_4	[4]	1.80–2.10	433–471	26, 31
$LiGaO_2$	[4]	1.95–2.00	415	27, 32
$LiNiPO_4$	[6]	2.097–2.148	396–529	33, 34
$LiMgPO_4$	[6]	2.098–2.174	290–559	34, 35

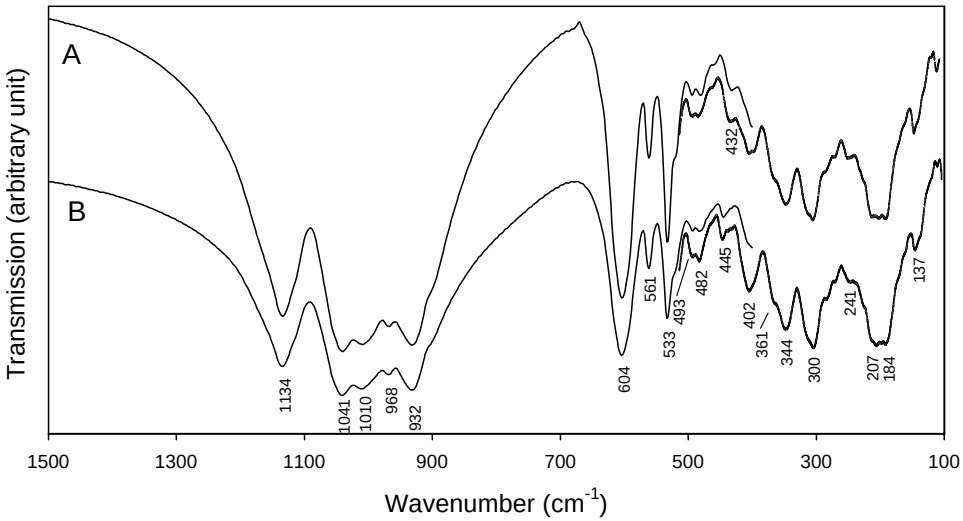

FIG. 5. Infrared spectra of $Na_{0.50}Li_{0.50}CdIn_2(PO_4)_3$ (A) and $Na_{0.50}{}^6Li_{0.50}CdIn_2(PO_4)_3$ (B).

densities involved in the $Na^+ \rightarrow Li^+$ substitution, lithium has not been accurately localized in the alluaudite-like compounds $(Na_{1-x}Li_x)CdIn_2(PO_4)_3$. Nevertheless, it seems evident from the Rietveld refinements that this cation occurs on the large $A(1)$ and/or $A(2)'$ crystallographic sites. It is important to note that the occurrence of lithium on large crystallographic sites is already mentioned in the literature, and is favored by a partial lithium occupancy (28).

The unit cell volume for $NaMnFe_2(PO_4)_3$ is 877.3(2) Å^3 (2), whereas, in contrast, the volume obtained herein for $NaCdIn_2(PO_4)_3$ is 963.7(3) Å^3 (Table 4). Thus, the replacement of Mn^{2+} and Fe^{3+} by Cd^{2+} and In^{3+}, respectively, implies an increase of nearly 10% of the unit cell volume. An important consequence of this larger unit cell is the significant increase in the $A(1)$–O and $A(2)'$–O bond distances, an increase which modifies the coordination polyhedra morphologies of $A(1)$ and $A(2)'$ sites. The distorted cube $A(1)$ and the gable disphenoid $A(2)'$ in $NaMnFe_2(PO_4)_3$ (2) become a distorted octahedron and a distorted trigonal prism in $NaCdIn_2(PO_4)_3$, respectively (Fig. 3). Because lithium generally accommodates small crystallographic sites (28), the incorporation of this cation on the $A(1)$ and/or $A(2)'$ sites of the alluaudite framework is also more limited in the $(Na_{1-x}Li_x)CdIn_2(PO_4)_3$ solid solution ($x = 0.55$), than in the $(Na_{1-x}Li_x)MnFe_2(PO_4)_3$ solid solution ($x = 0.90$) (2).

ACKNOWLEDGMENTS

The authors are indebted to Prof. G. J. Long, and to three anonymous reviewers, for constructive comments and critical reading of the earlier versions of this manuscript.

REFERENCES

1. P. B. Moore, *Am. Mineral.* **56,** 1955–1975 (1971).
2. F. Hatert, P. Keller, F. Lissner, D. Antenucci, and A.-M. Fransolet, *Eur. J. Mineral.* **12,** 847–857 (2000).
3. P. B. Moore and J. Ito, *Mineral. Mag.* **43,** 227–235 (1979).
4. D. Antenucci, Ph.D. Thesis, University of Liège, 1992.
5. D. Antenucci, G. Miehe, P. Tarte, W. W. Schmahl, and A.-M. Fransolet, *Eur. J. Mineral.* **5,** 207–213 (1993).
6. S. Khorari, A. Rulmont, R. Cahay, and P. Tarte, *J. Solid State Chem.* **118,** 267–273 (1995).
7. S. Khorari, A. Rulmont, and P. Tarte, *J. Solid State Chem.* **131,** 290–297 (1997).
8. S. Khorari, A. Rulmont, and P. Tarte, *J. Solid State Chem.* **134,** 31–37 (1997).
9. K.-H. Lii and J. Ye, *J. Solid State Chem.* **131,** 131–137 (1997).
10. T. E. Warner, W. Milius, and J. Maier, *J. Solid State Chem.* **106,** 301–309 (1993).
11. O. V. Yakubovich, M. A. Simonov, Yu. K. Egorov-Tismenko, and N. V. Belov, *Dokl. Akad. Nauk USSR* **236,** 1123–1126 (1977).
12. M. B. Korzenski, G. L. Schimek, J. W. Kolis, and G. J. Long, *J. Solid State Chem.* **139,** 152–160 (1998).
13. D. R. Corbin, J. F. Whitney, W. C. Fultz, G. D. Stucky, M. M. Eddy, and A. K. Cheetham, *Inorg. Chem.* **25**(14), 2279–2280 (1986).
14. K.-H. Lii and P.-F. Shih, *Inorg. Chem.* **33,** 3028–3031 (1994).
15. F. Leroux, A. Mar, C. Payen, D. Guyomard, A. Verbaere, and Y. Piffard, *J. Solid State Chem.* **115,** 240–246 (1995).
16. F. Leroux, A. Mar, D. Guyomard, and Y. Piffard, *J. Solid State Chem.* **117,** 206–212, (1995).
17. P. Keller, H. Riffel, F. Zettler, and H. Hess, *Z. Anorg. Allg. Chem.* **474,** 123–134, (1981).
18. S. Khorari, A. Rulmont, and P. Tarte, *J. Solid State Chem.* **137,** 112–118 (1998).
19. C. W. Burnham, "LCLSQ version 8.4, least-squares refinement of crystallographic lattice parameters." Dept. of Earth and Planetary Sciences, Harvard University, 1991.
20. J.-M. Winand, A. Rulmont, and P. Tarte, *J. Solid State Chem.* **87,** 83–94 (1990).

21. D. Antenucci, A.-M. Fransolet, G. Miehe, and P. Tarte, *Eur. J. Mineral.*, **7,** 175–181 (1995).
22. R. D. Shannon, *Acta Crystallogr. A* **32,** 751–767 (1976).
23. I. D. Brown and D. Altermatt, *Acta Crystallogr. B* **41,** 244–247 (1985).
24. R. P. Hermann, F. Hatert, A.-M. Fransolet, G. J. Long, and F. Grandjean, *J. Solid State Chem.* submitted October 2001.
25. P. Tarte, *Spectrochim. Acta* **20,** 238–240 (1964).
26. P. Tarte, *Spectrochim. Acta* **21,** 313–319 (1965).
27. P. Tarte, *Mém. Acad. Roy. Belgique, Cl. Sci.*, 8, 2*è sér.* **XXXV (4a, 4b),** 260 (1965).
28. M. Wenger and T. Armbruster, *Eur. J. Mineral.* **3,** 387–399 (1991).
29. R. A. Young, A. C. Larson, and C. O. Paiva-Santos, "User's guide to program DBWS-9807 for Rietveld analysis of X-ray and neutron powder diffraction patterns," p. 56. School of Physics, Georgia Institute of Technology, Atlanta, GA, 1998.
30. J. Zemann, *Acta Crystallogr.* **10,** 664–666 (1957).
31. W. H. Zachariasen and H. A. Plettinger, *Acta Crystallogr.* **14,** 229–230 (1961).
32. M. Marezio, *Acta Crystallogr.* **18,** 481–484 (1965).
33. I. Abrahams and K. S. Easson, *Acta Crystallogr. C* **49,** 925–926 (1993).
34. M. T. Pâques-Ledent and P. Tarte, *Spectrochim. Acta* **30A,** 673–689 (1974).
35. F. Hanic, M. Handlović, K. Burdová, and J. Majling, *Crystallogr. Spectrosc. Res.* **12(2),** 99–127 (1982).